Fast and robust position determination in the scanning electron microscope

Christian Dahmen and **Tobias Tiemerding**
Division of Microrobotics and Control Engineering
University of Oldenburg, Germany
christian.dahmen@uni-oldenburg.de

Abstract

This paper deals with the extraction of small object positions in the scanning electron microscope (SEM). An approach based on line scanning and new object tracking approaches are presented and evaluated for their capabilities to reliably track objects in the SEM when the objects are moving quickly. Image acquisition of such fast moving objects has the issue of strong distortions and very high displacements, which can affect the performance of the algorithms. The new approaches are compared to common image processing algorithms.

1 Introduction

Objects on the nanoscale e.g. carbon nanotubes (CNTs), nanowires or graphene-based samples have already attracted broad interest for industrial applications and the research community. Nanorobotic systems are a key technology for the characterization of these structures and the process of assembling [Eichhorn *et al.*, 2009]. Nanorobotic stages as a basic component are often used as a specimen holder and for both coarse and fine positioning of the examined nanorobotic materials [Zimmermann *et al.*, 2013; Bartenwerfer *et al.*, 2011]. To achieve high-throughput for industrial applications it is necessary to acquire precise position information of this tools and nanoobjects. In addition it is necessary to allow for relative positioning. However, as experience has shown, scanning electron microscope (SEM) is the only device that can be used to acquire these information. Here it is infeasible to rely only on sensors that are local to a single nanopositioner. These kind of sensors cannot be used because of adverse effects on the nanoscale, e.g drift, even if a significant calibration is applied.

SEM images have been applied successfully as a feedback in a variety of different setups for nanohandling [Wortmann *et al.*, 2009; Eichhorn *et al.*, 2008]. A wide variety of algorithms have been adapted for SEM image processing, e.g. cross correlation and active contours [Sievers *et al.*, 2006]. For both approaches the maximum movement speed is limited. For active contours, an object is not allowed to move out of the last known position by more than 50% between two consecutive images. For template based approaches, because of line-wise scanning there is a significant object distortion while moving. This implies an almost linear correlation score drop for increasing movement speeds. Object tracking with cross correlation becomes unreliable with speeds > 100 µm/s [Jasper *et al.*, 2011]. For closed-loop control in high throughput industrial applications this kind of image processing is insufficient. Here, approaches are evaluated which solve some of the mentioned problems.

Section 2 describes an approach for line scan based tracking in the SEM. In Section 3, image based tracking algorithms are presented. The algorithm performance is evaluated in Section 4. The paper concludes with a summary and outlook on future work in section 5.

2 Line Scan based Tracking

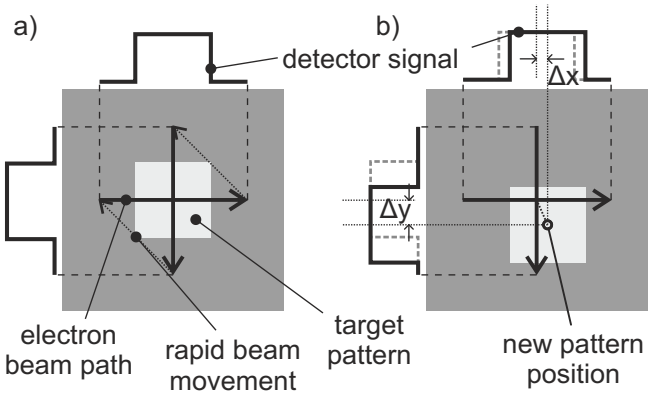

Figure 1: Scanning pattern for a square-shaped target: a) stationary and b) moving. The deviation of the detector signal between two line-scans is used to retrieve the movement in δx and δy. From [Jasper et al., 2011]

For this paper a silicon wafer with a rectangular pattern with a size of 1 µm^2 was used. Such a pattern can

be manufactured by using focused ion beam deposition [Volkert and Minor, 2007] (see Fig. 2). To detect the current position of a pattern two orthogonal line scans can be used, which have to be performed exactly over the last known position of the pattern [Jasper and Fatikow, 2010], [Jasper *et al.*, 2010], [Jasper *et al.*, 2011].

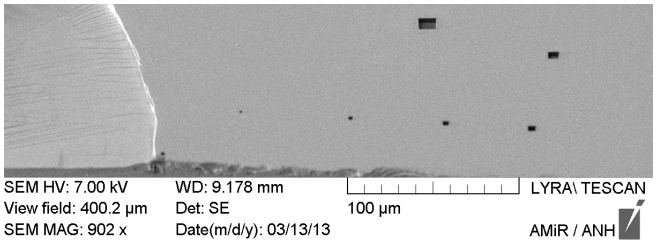

Figure 2: Patterns manufactured with focused ion beam deposition

While performing the two line scans the detector generates a square-wave signal as shown in Fig. 1. For a stationary object the wave is centered over the middle of the scan (see Fig. 1 a). In movement, the line scans are no longer conducted over the center of the pattern. This results in a deviation of the detector signal during a line scan (see Fig. 1 b). The deviation is used to calculate the movement offset Δx and Δy. In conjunction with the last known position of the pattern the new current position can be calculated. An initial position of the pattern, needed for the first position calculation, can be determined using visual feedback of the SEM and conventional object detection algorithms or detection using human perception. The following section 2.1 describes an implementation of this tracking approach. Achievable performance and potential problems will be analyzed in section 2.2.

2.1 Implementation using center of gravity calculation

Each line scan generates a detector signal generally similar to Fig. 1. These data can be used to determine the pattern position on the scanned line. One approach, presented in [Jasper and Fatikow, 2010], uses center of gravity (CoG) calculation. After weighting every pixel with its gray value, the center of gravity of these values is likely to represent the center of the pattern. On a line of length N with pixel values p_i the CoG c is calculated as follows:

$$c = \frac{\sum_{i=0}^{N-1} i \cdot p_i}{\sum_{i=0}^{N-1} p_i} = \frac{s_w}{s_v} \tag{1}$$

By using this calculation there are two disadvantages:

1. In object movement: The CoG no longer exactly represents the objects position because only a part of the object is on the scanned line (Fig. 3 b).

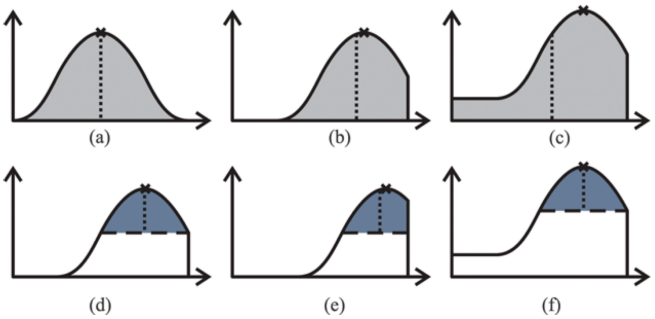

Figure 3: Several cases for determining the position of the object with CoGC. The dotted line represents the center of gravity, X is the exact position of the object and the dashed line the chosen threshold T. From [Jasper and Fatikow, 2010]

2. High sensitivity: Changes in pixel values, e.g. due to brightness changes of the SEM image, cause a alternating influence of pixels not belonging to the object which is tracked (Fig. 3 c).

A threshold function $t(p_i)$ can be applied to the pixel values before calculating the CoG to overcome the disadvantages (see Fig. 3 d). By adjusting the threshold T according to the scan the approach is robust against changes in brightness [Jasper and Fatikow, 2010]. The calculation is thus changing as follows:

$$\begin{aligned} c &= \frac{\sum_{i=0}^{N-1} i \cdot t(p_i)}{\sum_{i=0}^{N-1} p_i} \text{ with} \\ t(p_i) &= \begin{cases} 0 & \text{when } p_i < T \\ p_i - T & \text{else} \end{cases} \end{aligned} \tag{2}$$

2.2 Tracking performance

As described in [Jasper *et al.*, 2011] and [Jasper *et al.*, 2010] the movement of an object between two line scan iterations should not exceed 40% of the pattern size. Therefore a 1 µm^2 sized object allows for maximum movement distance is 400 nm between two line scans. As shown in [Jasper, 2009] tracking with an update rate of 1 kHz for resolutions less then 5 nm is theoretically possible. Thus allowing for maximum movement speeds of 400 µm / s.

In practice, the maximum movement speed is significant below the theory. This is due to the direct SEM sensing focussed to a small area of interest (here: lines). Each line scan over the pattern generates deposits. Fig. 4 b shows the change of the pattern environment due to deposits. This change evolved in about ten minutes of pattern tracking. The algorithm itself needs virtually binary input images, which are generated by thresholding the input (see Fig. 4 c and Fig. 4 d). It becomes obvious that the deposits distort the pattern and introduce

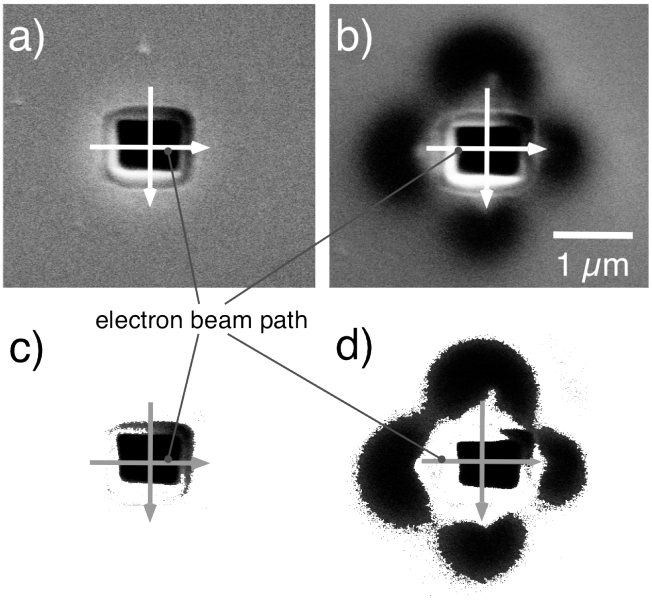

Figure 4: Deposits generated using SEM line scans (a and b). The thresholded images c and d are used as the input for the algorithm. The shown deposits evolved in about ten minutes of pattern tracking.

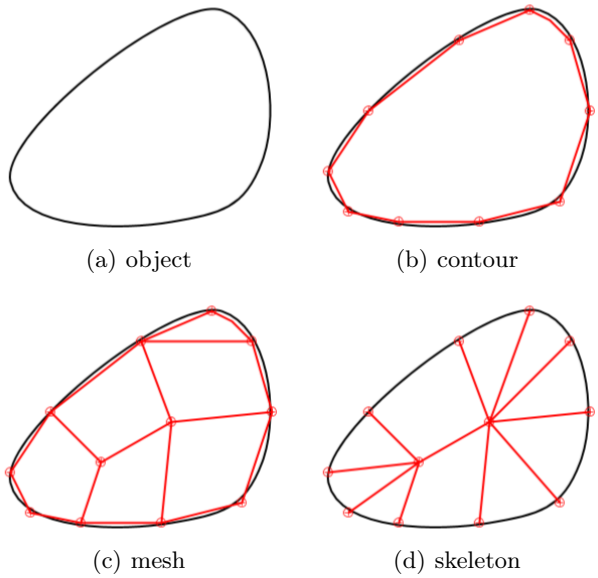

Figure 5: Different graph types implemented and used for the tracking algorithms.

a source of error. Especially in movement the deposits move into the scanning area and thus can lead to false calculations.

Therefore the maximum movement distance should be selected so that deposits do not enter the scanning area at any given time. The distance in this paper was thus set to 120 nm which leads to maximum movement speeds of 120 µm/s.

3 Image based Tracking Algorithms

A selection of algorithms has been implemented and compared with the linescan approach with respect to movement distortion. This includes active contours with distortion model, line template matching from [Dahmen and Fatikow, 2011] using a deformable skeleton and a mesh graph connecting SIFT features [Dahmen, 2012]. Additionally, standard template matching has been evaluated.

In Figure 5, the representations of the different graph models used are shown.

3.1 Template Matching

Standard template matching is used here. The approach has been used already in real microrobotic setups [Fatikow *et al.*, 2009]. It is based on cross correlation and uses templates or template images to determine regions with high similarity in an input image:

$$C = T \star I \tag{3}$$

with C the cross correlation matrix, T the template and I the image.

3.2 Active Contours

Active contours as proposed by Kass and Witkin [Kass *et al.*, 1988] have been used to segmentg foreground from background of an image.

Active contours are represented as polygons which delimit the object. An energy function belonging to the contour is minimized to segment the object. Restriction of the transformtions used for minimization make this a suitable algorithm for tracking [Sievers, 2007].

Active contours with free minimization are robust against deformations, but are sensible to many factors of influence which make it unstable to track objects. Also, the free minimization is computationally expensive.

Only euclidean transformations are used here to reduce the minimization effort [Sievers, 2007]. Additionally, shear transformations are added to allow better modelling of the distortions.

As explained in [Dahmen and Fatikow, 2011], movement in x-direction will lead to stronger distortions than movement in y-direction.

The energy function for the active contours according to [Fatikow *et al.*, 2009] are:

$$E_{int1} = \frac{L^3}{A} \tag{4}$$

with L the length of the contour, and A the enclosed

area, and

$$E_{ext} = N_a f\left(\frac{1}{N_a}\sum_{x\in a} x\right) + N_b f\left(\frac{1}{N_b}\sum_{x\in b} x\right) \quad (5)$$

with $f(z) = -zln(z)$ as external energy part.

The transformations assume a continuous motion. Speed changes during acquisition of the object will lead to more complex distortions which cannot be immediately covered. Analysis of the contour could deliver information about this, but the shape space in which minimization is done would be drastically increased.

3.3 SIFT mesh

Contours segment the object by its outer hull. A mesh on the other hand connects feature points not only over edges along the object boundary, but also inside the object. Also, features may be inside the object and not only on the contour.

Here, SIFT features [Lowe, 1999] are used to detect the tracked object. From a choice of SIFT features extracted in a detection step, the most significant ones are connected to a mesh. This mesh is then used and an energy function minimized with the goal of determining the object position. In each step, SIFT features are generated and collected. Filtering is done according to similarity with the mesh SIFT features and the least similar discarded. The mesh is matched on the remaining features with euclidean transformations and the deformation model.

The internal energy of the mesh is used as:

$$E_{int} = \frac{L^3}{A} \quad (6)$$

with

$$L = \sum_{e\in edges} l_e \quad (7)$$

A is the enclosed area of mesh.

The external energy is used as:

$$E_{ext} = \sum |\bar{x}_{feature} - \bar{x}_{contour}| \quad (8)$$

As shape transformations, translation, rotaton, scaling, shear in x-direction and stretching in y-direction are used, with

$$C_t = S_{shear} \cdot C \quad (9)$$

with

$$S_{shear} = \begin{pmatrix} 1 & s_{xshear} & 0 \\ 0 & 1 & 0 \\ 0 & 0 & 1 \end{pmatrix} \quad (10)$$

$$C_t = S_{stretch} \cdot C \quad (11)$$

with

$$S_{stretch} = \begin{pmatrix} 1 & 0 & 0 \\ 0 & s_{ystretch} & 0 \\ 0 & 0 & 1 \end{pmatrix} \quad (12)$$

3.4 Line Template Skeleton

The line template skeleton based approach is taken from the approach in [Dahmen and Fatikow, 2011]. Instead of free minimization, a rigid model with deformation transformations is used.

The energy functions used for the minimization are:

$$\vec{E_1} = a \cdot (\vec{X_n} - \vec{X_{nmax}})^2 \quad (13)$$

with a a weighting factor, $\vec{X_n}$ the position of the skeleton point n, X_{nmax} the determined position of the line template n, and

$$\vec{E_2} = b \cdot ((\vec{X_n} - \vec{X_{n-1}} + d\vec{X})^2 + (\vec{X_n} - \vec{X_{n+1}} - d\vec{X})^2) \quad (14)$$

with b a weighting factor, $\vec{X_{n-1}}$ the position of the previous skeleton point, $\vec{X_{n+1}}$ the position of the next skeleton point and $d\vec{X}$ the original vector between the skeleton points in static case.

Using these energy functions and the transformation functions introduced before, the skeleton is able to deform to match the distorted object.

4 Evaluation

To compare the performance of the different algorithms with the linescan based approach, a setup has been used to move the pattern seen in Figure 6 in different speeds. The slowest speed was around 100 pixel per second, up to 10000 pixel per second, at an acquisition speed of the SEM of 6 frames per second. Each movement was repeated 100 times and tracking initialized before each run. The tracking failures were and the possible tracking recoveries after short tracking failure were recorded.

The active contours approach was only able to track in slow speeds. Faster movements lead to tracking loss and the algorithm cannot recover from that.

Template matching in this case worked up to higher speeds, and was able to recover from tracking failure. Failure occurred starting from 1100 pixel per second. Starting from 2000 pixel per second, the algorithm lost the tracking completely predictably, but was able to recover in steady state.

The linescan based approach was able to track the pattern up to a speed of around 5000 pixel per second without too frequent tracking loss. Tracking loss started to occur sometimes starting from 3600 pixel per second. The line template skeleton and SIFT mesh algorithms had tracking failures earlier, starting at around 2000 pixel per second, but in contrast to the linescan based approach, the algorithms recovered tracking as soon as the distortion reduced in steady state. The linescan based approach was not able to recover lost tracking.

Table 1: Tracking performance of the algorithms on the markers with different speeds

Algorithm	Speed kPix/s	Robustness	Recovery
Active contours	0.1	++	o
	0.6	-	- -
	1.1	- -	- -
	1.6	- -	- -
	2.1	- -	- -
	2.6	- -	- -
	3.1	- -	- -
	>3.6	- -	- -
Template	0.1	++	o
	0.6	++	o
	1.1	+	++
	1.6	-	++
	2.1	- -	++
	2.6	- -	++
	3.1	- -	++
	>3.6	- -	++
Skeleton with Line Templates	0.1	++	o
	0.6	++	o
	1.1	++	++
	1.6	++	++
	2.1	+	++
	2.6	-	++
	3.1	- -	++
	>3.6	- -	++
Mesh with SIFT features	0.1	++	o
	0.6	++	o
	1.1	++	o
	1.6	++	o
	2.1	-	++
	2.6	- -	++
	3.1	- -	++
	>3.6	- -	++
Linescan based approach	0.1	++	o
	0.6	++	o
	1.1	++	o
	1.6	++	o
	2.1	++	o
	2.6	++	o
	3.1	++	o
	3.6	+	- -
	4.1	+	- -
	4.6	+	- -
	5.1	-	- -
	5.6	-	- -
	6.1	-	- -
	6.6	-	- -
	7.1	- -	- -
	>7.6	- -	- -

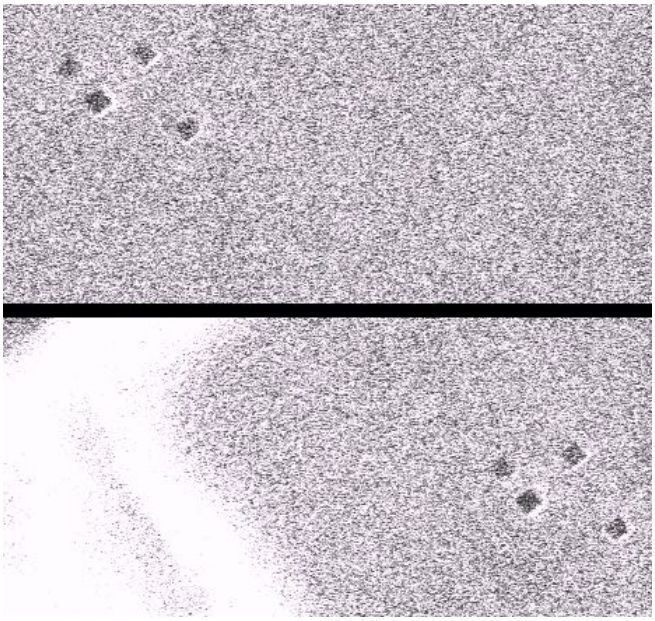

Figure 6: Pattern used for comparison with linescan based approach. Top: left position of the pattern. Bottom: right position of the pattern.

5 Summary and Outlook

The approaches presented in this paper can be used to track objects in fast movement in the SEM, specifically the line scan based tracking and the SIFT mesh and line template based tracking. As has been shown here, the proposed algorithms for line template matching and SIFT mesh tracking deliver reliable results on moving distorted objects tracked in SEM images. While template matching itself can still work up to a certain deformation, it fails when deformation is too strong. Reducing the template size is not an alternative option, as this increases ambiguities and makes the tracking very unstable. Active Contours with additional deformation modelling might track deformed objects, but fail in practice due to the big displacements from one frame to the next. Overall the SIFT mesh and line template skeleton seem to be reasonable approaches to deal with motion distortion in SEM images.

While the image based approaches have advantages considering reinitialization of the object after tracking loss, the line scan based approach is able to track faster motions and motion over a greater range without the additional issues introduced by image acquisition.

Most important for the future is that the problem of deposits during a line scan has to be solved. One approach may include the usage of different tracking patterns. In following evaluations, the image based algorithms have to be optimized and the capabilities for strong non-continuous movement tracking have to be

analyzed. The used line scan based tracking approach can be taken to application like high-speed control of a cantilever for an atomic force microscope (AFM) in the future.

References

[Bartenwerfer *et al.*, 2011] M. Bartenwerfer, V. Eichhorn, D. Jasper, S. Fatikow, A. Savenko, D. H. Petersen, B. Malm, and P. Bøggild. Automated Handling and Assembly of Customizable AFM-Tips. In *Proceedings of the IEEE International Symposium on Assembly and Manufacturing (ISAM'11)*, pages 1–6, Tampere, Finland, May 25-27 2011.

[Dahmen and Fatikow, 2011] Christian Dahmen and Sergej Fatikow. Tracking of objects in motion-distorted scanning electron microscope images. In *Intelligent Robots and Systems (IROS), 2011 IEEE/RSJ International Conference on*, pages 19 –24, September 2011.

[Dahmen, 2012] Christian Dahmen. Robust tracking of motion-distorted objects using active models. In *Optomechatronic Technologies (ISOT), 2012 International Symposium on*, pages 1–6. IEEE, 2012.

[Eichhorn *et al.*, 2008] V. Eichhorn, S. Fatikow, C. Dahmen, C. Edeler, C. Stolle, and D. Jasper. Automated Microfactory inside a Scanning Electron Microscope. In *Proc. of the 6th International Workshop on Microfactories (IWMF)*, pages 207–212, Evanston, Illinois, USA, October 5-7 2008.

[Eichhorn *et al.*, 2009] V. Eichhorn, S. Fatikow, T. Wortmann, C. Stolle, C. Edeler, D. Jasper, O. Sardan, P Bøggild, G. Boetsch, C. Canales, and R. Clavel. NanoLab: A Nanorobotic System for Automated Pick-and-Place Handling and Characterization of CNTs. In *Proceedings of the IEEE International Conference on Robotics and Automation (ICRA'09)*, pages 1826–1831, Kobe, Japan, May 12-17 2009.

[Fatikow *et al.*, 2009] S. Fatikow, C. Dahmen, T. Wortmann, and R. Tunnell. Vision feedback for automated nanohandling. In *Information and Automation, 2009. ICIA '09. International Conference on*, pages 806 – 811, June 2009.

[Jasper and Fatikow, 2010] Daniel Jasper and Sergej Fatikow. Line Scan-based High-Speed Position Tracking inside the SEM. *International Journal of Optomechatronics*, 4(2):115–135, June 2010.

[Jasper *et al.*, 2010] Daniel Jasper, Christoph Edeler, Claas Diederichs, and Sergej Fatikow. High-speed nanorobot position control inside a scanning electron microscope. In *Proc. of Electrical Engineering/Electronics, Computer, Telecommunications and Information Technology Conference*, pages 542–546, Chiang Mai, Thailand, May 2010. Best Paper Award.

[Jasper *et al.*, 2011] Daniel Jasper, Claas Diederichs, Christoph Edeler, and Sergej Fatikow. High-speed nanorobot position control inside a scanning electron microscope. *ECTI Transactions on Electrical Eng., Electronics, and Communications*, 9(1):177–186, Feburary 2011.

[Jasper, 2009] Daniel Jasper. High-speed Position Tracking for Nanohandling inside Scanning Electron Microscopes. In *Proc. of IEEE Intl. Conference on Robotics and Automation (ICRA)*, pages 508–513, Kobe, Japan, May 2009.

[Kass *et al.*, 1988] Michael Kass, Andrew Witkin, and Demetri Terzopoulos. Snakes: Active contour models. *International Journal of Computer Vision*, 1(4):321–331, 1988.

[Lowe, 1999] David G Lowe. Object recognition from local scale-invariant features. In *Computer vision, 1999. The proceedings of the seventh IEEE international conference on*, volume 2, pages 1150–1157. Ieee, 1999.

[Sievers *et al.*, 2006] Torsten Sievers, Marco Jähnisch, Christian Schrader, and Sergej Fatikow. Vision feedback in an automatic nanohandling station inside an SEM. *Optomechatronic Micro/Nano Devices and Components II*, 6376(1):63760B, 2006.

[Sievers, 2007] T. Sievers. Global sensor feedback for automatic nanohandling inside a scanning electron microscope. In *Intelligent production machines and systems: 2nd I* PROMS Virtual Conference, 3-14 July 2006*, page 289, 2007.

[Volkert and Minor, 2007] C. A. Volkert and A. M. Minor. Focused ion beam microscopy and micromachining. *MRS Bulletin*, 32:389–399, 4 2007.

[Wortmann *et al.*, 2009] T. Wortmann, C. Dahmen, R. Tunnell, and S. Fatikow. Image processing architecture for real-time micro-and nanohandling applications. In *Proc. of the Eleventh IAPR Conference on Machine Vision Applications (MVA)*, 2009.

[Zimmermann *et al.*, 2013] Sören Zimmermann, Tobias Tiemerding, Sergej Fatikow, W. Wang, T. Li, and Y. Wang. Automated mechanical characterization of 2D materials using SEM based visual servoing. March 2013.